Reconstructing H(z) from Spiral Geometry and Rotation Curves Without Dark Matter

E.P.J. de Haas[1, a)]

Kandinsky College, Nijmegen, The Netherlands

We introduce a new method for empirically determining the cosmic expansion history $H(z)$ using galactic structure alone, based on a gravitational metric inflow framework that does not require dark matter halos. In this model, both spiral arm geometry and galaxy rotation curves arise naturally from the motion of spacetime itself, driven by a central gravitational mass and the Hubble parameter at the time of structure formation. We derive analytical expressions for the effective orbital velocity and pitch angle of the inflowing metric, demonstrating that these quantities encode the value of $H(z)$ directly. By fitting observed rotation curves and spiral geometries from well-resolved galaxies, one can potentially extract empirical $H(z)$ estimates and compare them to standard ΛCDM predictions. Unlike traditional chronometers or BAO measurements, our approach relies solely on observed galaxy morphology and redshift, enabling a scalable and purely geometric reconstruction of the expansion history. We estimate that future surveys could yield 10^5 to 10^6 independent $H(z)$ measurements using this method, offering a powerful new observational test of cosmology and gravity.

Keywords: alternative gravity theory, quantum gravity, space quantisation, Dark Matter, Dark Energie, Hubble expansion

[a)]Electronic mail: haas2u@gmail.com

I. INTRODUCTION

In this paper we combine the idea of galactic dynamics as presented in [1; 3] with the principle that the Hubble expansion puts an effective limit on the reach of Newtonian gravitation, as presented in [4]. In a previous paper we presented what can be seen as a first iteration of the idea that the Hubble parameter Hz fundamentally influences galactic dynamics throughout the different epochs of the cosmos [2].

In [2] we claimed that galactic spirals contained a frozen memory of cosmic epochs through the constrained of the time dependent Hubble expansion on the Newtonian gravitational potential. The claim was based on a simple idea and intuition that the critical distance, as presented in [4], in its time dependent form with H_z instead of H_0, loosened galactic spirals and reduced their extend in space. But we worked it out too hasty. We didn't, for example, change the final velocity of galactic rotation curves. And we didn't realize that the idea automatically applied to the galactic rotation curves as well. The dependence of galactic rotation curves on the Hubble parameter is even more significant than the dependence of the spirals, because those rotation curves are easier quantifiable than the exact form of the galactic spirals.

In this paper we will work out these ideas more thorough, as its second iteration. One of the new ideas presented in this paper is that galactic bars in spiral disk galaxies are themselves spirals. Galactic bars are, in our opinion, time-frozen high z compact spirals nested in low(er) z large spirals. But let us start with the derivation of the correct metric velocities $\vec{v}_{rad} = v_{rad}\hat{r}$, $\vec{v}_{orb} = v_{orb}\hat{\varphi}$ and $\vec{v}_L = \vec{v}_{orb} + \vec{v}_{rad}$, and the correct spiral pitch angle $\alpha = \frac{v_{rad}}{v_{orb}}$, as corrected for the Hubble expansion influence. That brings us to another error in our first iteration: our spiral pitch angle α is r dependent. It has no relation at all with the spiral pitch angle used in the literature that is obtained through a logarithmic function and has one single value for the entire spiral. The logarithmic pitch angle is a purely geometric product, while ours is derived from galactic metric dynamics.

II. EXTRACTING $H(z)$ FROM GALACTIC ROTATION CURVES.

A. Effective Potential for $r \leq R$

We start from the classical potential per unit mass inside a uniform-density bulge and want to adjust this for the Hubble expansion putting a limit to the effective Newtonian reach.

$$\frac{V(r)}{m} = -\frac{GM}{2R}\left(3 - \frac{r^2}{R^2}\right)$$

First we convert this to a radial inflow velocity, using the kinetic energy equivalence:

$$\frac{1}{2}v_{\text{rad}}^2(r) = -\frac{V(r)}{m} \quad \Rightarrow \quad v_{\text{rad}}(r) = \sqrt{\frac{2GM}{2R}\left(3 - \frac{r^2}{R^2}\right)} = \sqrt{\frac{GM}{R}\left(3 - \frac{r^2}{R^2}\right)}$$

We then subtract the Hubble expansion velocity and define the effective intrinsic radial velocity of space

$$v_{\text{rad,eff}}(r, Hz) = v_{\text{rad}}(r) - v_{Hz} = v_{\text{rad}}(r) - H_z r,$$

and then convert this back to a modified potential energy. For this we again use the kinetic energy to potential relation through the escape velocity procedure:

$$\frac{1}{2}v_{\text{rad,eff}}^2(r, Hz) = -\frac{V_{\text{eff}}(r, Hz)}{m} \quad \Rightarrow \quad \frac{V_{\text{eff}}(r, Hz)}{m} = -\frac{1}{2}\left(v_{\text{rad}}(r) - H_z r\right)^2$$

The final result is:

$$\frac{V_{\text{eff}}(r, Hz)}{m} = -\frac{1}{2}\left(\sqrt{\frac{GM}{R}\left(3 - \frac{r^2}{R^2}\right)} - H_z r\right)^2 = \frac{1}{2}v_{rad,eff}^2(r, Hz)$$

so we also have

$$v_{rad,eff}^2(r, Hz) = \left(\sqrt{\frac{GM}{R}\left(3 - \frac{r^2}{R^2}\right)} - H_z r\right)^2.$$

For $r = R$ we then get

$$\frac{V_{\text{eff}}(r, Hz)}{m} = -\frac{1}{2}\left(\sqrt{\frac{2GM}{R}} - H_z R\right)^2 = \frac{1}{2}v_{rad,eff}^2(R, Hz)$$

so

$$v_{rad,eff}^2(R, Hz) = \left(\sqrt{\frac{2GM}{R}} - RH_z\right)^2.$$

And for $r = 0$, we get

$$v_{rad,eff}^2(0, Hz) = \frac{3GM}{R} = \frac{3}{2}v_{esc}^2.$$

B. Effective Potential for $r \geq R$

We define outer effective potential per unit mass in the same way through the intermediary of the velocities of space::

$$\frac{V_{\text{eff}}(r,Hz)}{m} = -\frac{1}{2}\left(v_{esc} - v_H\right)^2 = -\frac{1}{2}\left(\sqrt{\frac{2GM}{r}} - H_z r\right)^2$$

which at $r = R$ can be valuated as:

$$\frac{V_{\text{eff}}(R,Hz)}{m} = -\frac{1}{2}\left(\sqrt{\frac{2GM}{R}} - H_z R\right)^2$$

and gives the same result as the inner effective potential energy. We define $r_c = r$ as the distance at which $v_{esc} = v_H$, so where $V_{eff} = 0$.

C. The Virial Theorem applied to the efffective potential energy at the edge of the bulge

We use the virial theorem at $r = R$ for a circular orbit in an effective potential and use it for the metric instead of material particles and we only use it at the boundary between bulge and disk:

$$K_{orb} = -\frac{1}{2}V_{\text{eff}}(R) \quad \Rightarrow \quad \frac{1}{2}mv_{\text{orb}}^2 = -\frac{1}{2}V_{\text{eff}}(R) \quad \Rightarrow \quad v_{\text{orb}}^2 = -\frac{V_{\text{eff}}(R)}{m}$$

From the outside in, we arrive at R from above We use the earlier expression for the effective potential outside the bulge:

$$\frac{V_{\text{eff}}(R)}{m} = -\frac{1}{2}\left(\sqrt{\frac{2GM}{R}} - H_z R\right)^2$$

so

$$v_{orb}^2 = -\frac{V_{\text{eff}}(R)}{m} = \frac{1}{2}\left(\sqrt{\frac{2GM}{R}} - H_z R\right)^2$$

We recall the Lagrangian definition to be:

$$L = K_{orb} - V_{\text{eff}} = \frac{1}{2}mv_{\text{orb}}^2 - V_{\text{eff}}(R)$$

We now substitute $v_{\text{orb}}^2 = -\frac{V_{\text{eff}}(R)}{m}$:

$$L = \frac{1}{2}m\left(-\frac{V_{\text{eff}}(R)}{m}\right) - V_{\text{eff}}(R) = -\frac{1}{2}V_{\text{eff}}(R) - V_{\text{eff}}(R) = -\frac{3}{2}V_{\text{eff}}(R)$$

In short, we have

$$L(R,Hz) = -\frac{3}{2}V_{\text{eff}}(R)$$

We use the earlier expression for the effective potential:

$$\frac{V_{\text{eff}}(R)}{m} = -\frac{1}{2}\left(\sqrt{\frac{2GM}{R}} - H_z R\right)^2$$

in terms of the velocity of space, the square of the Lagrangian velocity becomes:

$$\frac{2L}{m} = v_L = -3\cdot\left(\frac{V_{\text{eff}}(R)}{m}\right) = -3\cdot\left[-\frac{1}{2}\left(\sqrt{\frac{2GM}{R}} - H_z R\right)^2\right] = \frac{3}{2}\left(\sqrt{\frac{2GM}{R}} - H_z R\right)^2$$

This gives the new Lagrangian velocity at R, assuming:

- The orbit at $r = R$ is virialized with respect to the effective potential V_{eff},
- The standard definition $L = K - V$ holds at R.

D. The orbital velocity and Lagrangian inside the bulge

In a previous version of the galactic rotation curves, I constructed a model galaxy with a model bulge with mass M and radius R and an empty space around it. In such a mode galaxy, the Newtonian gravitational potential was fully determined by the bulge. The model bulge has constant density $\rho_0 = \frac{M}{V} = \frac{3M}{4\pi R^3}$ and its composing stars rotate on geodetics in a quasi-solid way. So all those stars in the bulge have equal angular velocity ω on their geodetic orbits, with $v_{orbit} = \omega r$. So we had $v_{orbit}^2 = \omega^2 r^2$ and

$$\frac{K_{orbit}}{m} = \frac{\omega^2 r^2}{2} \tag{1}$$

On the boundary between the quasi solid spherical bulge and the emptiness outside of it, the orbital velocities are behaving smoothly. So the last star in the bulge and the first star in the region outside of the bulge have equal velocities and potentials. This allows us to determine ω as in

$$\omega_{orb}^2 = \frac{v_{orb}^2(R)}{R^2} = -\frac{V_{\text{eff}}(R)}{mR^2} = \frac{1}{2R^2}\left(\sqrt{\frac{2GM}{R}} - H_z R\right)^2$$

So we get

$$v_{orb}^2(r) = \omega_{orb}^2 r^2 = \frac{v_{orb}^2(R)r^2}{R^2} = -\frac{V_{\text{eff}}(R)r^2}{mR^2} = \frac{1}{2}\left(\sqrt{\frac{2GM}{R}} - H_z R\right)^2 \frac{r^2}{R^2}$$

We can then determine $L(r)$ inside the bulge because $L(r) = K_{orb}(r) + K_{rad,eff}(r)$, so

$$\frac{2L}{m}(r) = v_{orb}^2(r) + v_{rad,eff}^2(r) = \frac{1}{2}\left(\sqrt{\frac{2GM}{R}} - H_z R\right)^2 \frac{r^2}{R^2} + \left(\sqrt{\frac{GM}{R}\left(3 - \frac{r^2}{R^2}\right)} - H_z r\right)^2.$$

As a result, inside such a model bulge, L is a not constant of the motion of the metric any more.

E. Orbital Velocity for $r > R$

We again postulate that the Lagrangian is constant in the whole disk. For $r > R$, the effective potential is:

$$\frac{V_{\text{eff}}(r)}{m} = -\frac{1}{2}\left(\sqrt{\frac{2GM}{r}} - H_z r\right)^2$$

We define the Lagrangian per unit mass outside the bulge as:

$$\frac{L}{m} = \frac{K_{orb}}{m} + \frac{K_{rad}}{m} = \frac{1}{2}v_{\text{orb}}^2 + \frac{1}{2}\left(\sqrt{\frac{2GM}{r}} - H_z r\right)^2$$

Substitute the conserved value of $\frac{L}{m}$:

$$\frac{1}{2}v_{\text{orb}}^2 + \frac{1}{2}\left(\sqrt{\frac{2GM}{r}} - H_z r\right)^2 = \frac{3}{4}\left(\sqrt{\frac{2GM}{R}} - H_z R\right)^2$$

Solve for v_{orb}^2:

$$v_{\text{orb}}^2 = \frac{3}{2}\left(\sqrt{\frac{2GM}{R}} - H_z R\right)^2 - \left(\sqrt{\frac{2GM}{r}} - H_z r\right)^2.$$

In brief, we have

$$v_{\text{orb}}^2 = \frac{3}{2}v_{rad,eff}^2(R) - v_{rad,eff}^2(r).$$

And for $v_{final,eff} = v_L$ we get

$$v_{\text{final, eff}}^2 = \frac{3}{2}v_{rad,eff}^2(R) = \frac{3}{2}\left(\sqrt{\frac{2GM}{R}} - H_z R\right)^2$$

F. Summary of results

1. *The effective values* inside *the bulge*

$$v_{orb}^2(r) = \frac{1}{2}\left(\sqrt{\frac{2GM}{R}} - H_z R\right)^2 \frac{r^2}{R^2}$$

$$v_{rad,eff}^2(r,Hz) = \left(\sqrt{\frac{GM}{R}\left(3-\frac{r^2}{R^2}\right)} - H_z r\right)^2 .$$

$$v_L^2(r) = \frac{1}{2}\left(\sqrt{\frac{2GM}{R}} - H_z R\right)^2 \frac{r^2}{R^2} + \left(\sqrt{\frac{GM}{R}\left(3-\frac{r^2}{R^2}\right)} - H_z r\right)^2 .$$

2. *The effective values* outside *the bulge*

$$v_{\rm orb}^2 = \frac{3}{2}\left(\sqrt{\frac{2GM}{R}} - H_z R\right)^2 - \left(\sqrt{\frac{2GM}{r}} - H_z r\right)^2 .$$

$$v_{rad,eff}^2 = \left(\sqrt{\frac{2GM}{r}} - H_z r\right)^2 .$$

$$v_L^2 = v_{final}^2 = \frac{3}{2}\left(\sqrt{\frac{2GM}{R}} - H_z R\right)^2$$

3. *The new spiral pitch angle outside the bulge*

$$tan(\alpha_L) = \frac{|v_{rad,eff}|}{|v_{orb}|} = \frac{\sqrt{\frac{2GM}{r}} - H_z r}{\sqrt{\left[\frac{3}{2}\left(\sqrt{\frac{2GM}{R}} - H_z R\right)^2 - \left(\sqrt{\frac{2GM}{r}} - H_z r\right)^2\right]}}$$

$$\vec{v}_L = \vec{v}_{orb} + \vec{v}_{rad,eff}$$

$$\vec{v}_{rad,eff} = -v_{rad,eff}\hat{r} = -\left(\sqrt{\frac{2GM}{r}} - H_z r\right)\hat{r}$$

$$\vec{v}_{orb} = v_{orb}\hat{\varphi} = \sqrt{\left(\frac{3}{2}\left(\sqrt{\frac{2GM}{R}} - H_z R\right)^2 - \left(\sqrt{\frac{2GM}{r}} - H_z r\right)\right)}\hat{\varphi}$$

$$\vec{v}_L = \vec{v}_{orb} + \vec{v}_{rad}$$

$$v_L^2 = v_{orb}^2 + v_{rad,eff}^2$$

In appendix (A), we plotted spirals for a standard bulge at different z and we included a graph of r_c against cosmic time.

III. DYNAMICS OF ROTATION CURVES AND SPIRAL ARMS IN THE CONSTANT LAGRANGIAN METRIC APPROACH

In previous work, I developed a new theory of galactic spiral dynamics based on a constant metric Lagrangian [2]. This work was a continuation of my work on galactic rotation curves [1], were I fitted galaxy rotation curves on the constant Lagrangian curve. These works had the velocity of space theory of gravity as background, a metric theory of gravity that had one of its foundations in Hubble space expansion, as I elaborated earlier, see [3] and the references therein. I then realized that the combination of these works led to a new way to determine the Hubble constant from galactic spiral morphology, which I published in a short sketch [4]. For that paper I used, for the first time, ChatGPT as scientific assistent and I wasn't that aware yet of the pitfalls of this marvellous AI program. The present paper is an elaboration of that short sketch and includes some corrections regarding pitch angle measurement, which aren't needed at all because the geometric spiral fit will do to retrieve Hz.

IV. ROTATION CURVES AS PROBES OF THE HUBBLE PARAMETER $H(z)$

In the standard cosmological model, galaxy rotation curves are interpreted through the lens of Newtonian dynamics embedded in a dark matter halo. Flat or rising rotation curves at large radii are attributed to massive, invisible dark matter halos that extend well beyond the luminous matter.

In contrast, the gravitational metric inflow model introduces an alternative explanation, in which the inflow of the spacetime metric itself governs the orbital motion of matter. In this framework, the orbital velocity of spacetime at a given radius is determined by both the central gravitational mass and the cosmic expansion rate at the time the structure formed. The orbital velocity is given by:

$$v_{\rm orb}^2(r) = \frac{3}{2}\left(\sqrt{\frac{2GM}{R}} - H_z R\right)^2 - \left(\sqrt{\frac{2GM}{r}} - H_z r\right)^2, \tag{2}$$

where M is the central (bulge) mass, R is a reference radius (typically the bulge radius), r is the radial distance from the center, and H_z is the Hubble parameter at the epoch of structure formation. For the outer spiral of galaxies this is the epoch of light emission.

This formula encapsulates both gravitational and cosmological dynamics without invoking dark matter. Notably, the shape of the rotation curve depends sensitively on H_z, which opens the possibility of using rotation curves as direct cosmological probes.

A. Methodology

Given a galaxy with a well-measured rotation curve $v_{\rm obs}(r)$, and a reasonable estimate of the central bulge mass M, one can numerically invert Eq. (2) to fit for the value of H_z that best reproduces the observed curve. The steps are:

1. Collect rotation curve data from optical or HI observations.
2. Estimate the central mass M and reference radius R from stellar light or kinematics.
3. Use Eq. (2) to fit $v_{\rm orb}(r)$ to the data, treating H_z (and optionally M and R) as free parameters.
4. Derive the best-fit value of H_z corresponding to the formation epoch of that spiral structure.

This approach allows one to empirically derive the Hubble parameter $H(z)$ from individual galaxies, independent of standard cosmological assumptions.

B. Advantages Over Traditional Methods

Traditional methods to measure $H(z)$, such as cosmic chronometers, baryon acoustic oscillations (BAO), and gravitational lensing time delays, are limited by statistical noise, indirect modeling, and sparse redshift coverage. In contrast, the rotation curve method offers:

- Direct extraction of H_z from galaxy dynamics.
- High statistical potential: thousands to millions of spiral galaxies with usable data.
- Applicability across a broad redshift range ($z = 0$ to $z \sim 6$).
- No dependence on dark matter assumptions or standard candles.

Thus, rotation curves serve not only as diagnostic tools for galactic structure but also as precision probes of cosmological expansion within the metric inflow paradigm.

V. SELF-ORGANIZED NESTED SPIRAL FORMATION FROM METRIC INFLOW

A. The original bulge as primal seed for the first spiral growth

In the gravitational metric inflow model, the onset of spiral structure is determined by the expansion of the inflow region around a seed mass to a physically relevant scale. This region is bounded by the critical radius r_c, defined as

$$r_c(z) = \left(\frac{2GM}{H(z)^2} \right)^{1/3}, \tag{3}$$

where M is the enclosed central mass and $H(z)$ is the Hubble parameter at redshift z.

The first appearance of spiral structure corresponds to the epoch when r_c becomes large enough (typically ~ 1 kpc) to entrain significant baryonic gas along a spiral trajectory. For a minimal seed mass of 1×10^{38} kg, this threshold is reached at $z \approx 66$, or approximately 31 million years after the Big Bang. At this point, the seed's gravitational metric inflow establishes the foundation for spiral-driven mass accretion.

As cosmic time progresses, the ambient baryonic density decreases, but the inflow region expands due to two factors:

1. Continuous accretion of gas by the inward-moving metric increases the central mass.

2. The Hubble parameter $H(z)$ decreases, expanding r_c even without additional mass.

This dynamic creates a feedback loop where inflow drives mass growth, which in turn expands the inflow region. Figure 1 shows how the critical radius (and thus the effective bulge radius) grows from 1 kpc at $z = 66$ to over 2 kpc by $z = 2$, purely from this self-sustaining mechanism.

This growth sets the stage for the emergence of successive spiral layers, each forming at later epochs around the expanded bulge. The next subsection explores how this initial mass foundation gives rise to nested spiral structures, entirely within the framework of gravitational metric inflow.

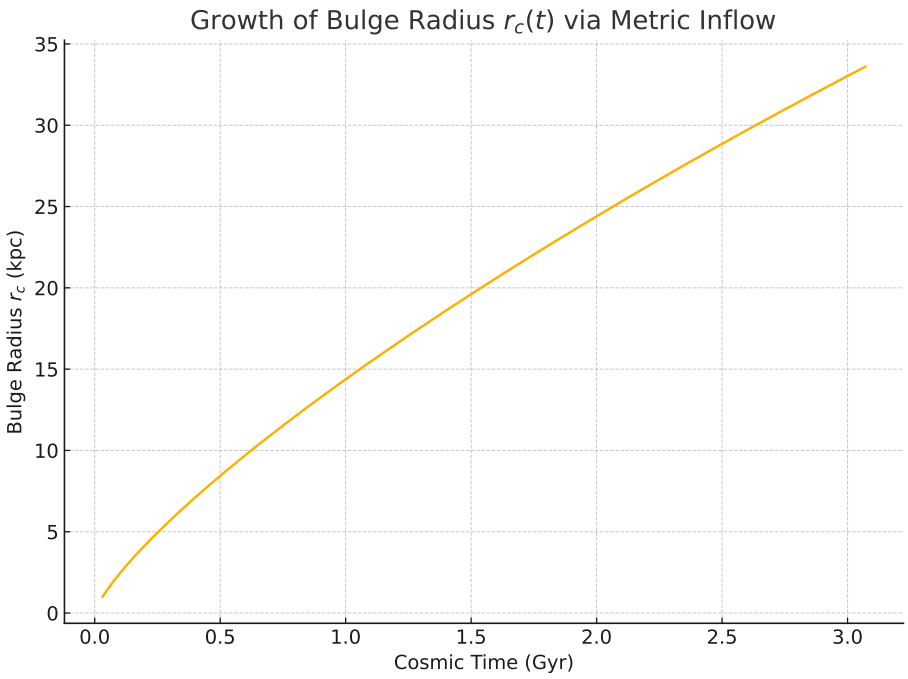

FIG. 1. Time evolution of the bulge radius $r_c(t)$ due to gravitational metric inflow, starting from an initial seed mass of 1×10^{38} kg at redshift $z \approx 66$. The critical radius r_c, which defines the boundary of the gravitational inflow region, also determines the effective bulge radius in this model. As the metric inflow carries ambient gas inward, the central mass grows, and with the decreasing Hubble parameter $H(z)$, the critical radius expands accordingly. This figure shows how the bulge radius increases from $r_c \approx 1\,\mathrm{kpc}$ at $z = 66$ to over $2\,\mathrm{kpc}$ by $z = 2$, forming the structural foundation for nested spiral development without requiring mergers or cold dark matter halos.

B. Gravitational Inflow as Metric Motion

In this framework, gravitational attraction is not treated as a force within static space, but as the result of a metric inflow: space itself moves inward toward a central mass concentration. The effective radial velocity of this gravitational inflow is described by

$$\vec{v}_{\mathrm{rad,eff}}(r) = -\left(\sqrt{\frac{2GM(r)}{r}} - H(z)\,r\right)\hat{r}, \tag{4}$$

where G is Newton's constant, $M(r)$ is the enclosed mass, and $H(z)$ is the Hubble parameter at redshift z.

In addition to the radial component, the inflow also includes an intrinsic azimuthal (orbital) component, such that the total flow follows a spiral trajectory. This spiral nature is not derived

from classical angular momentum conservation but is postulated as part of a constant Lagrangian metric inflow: the metric carries space and matter inward along spiral paths with constant local velocity magnitudes. The justification for this postulate lies outside the scope of this work and is left to future developments in theoretical physics.

C. Feedback Mechanism and Critical Radius

The flow boundary is set by the critical radius,

$$r_c(z) = \left(\frac{2GM}{H(z)^2} \right)^{1/3}, \tag{5}$$

which delineates the region within which gravitational inflow dominates over cosmological expansion. This critical radius evolves naturally over time: as $H(z)$ decreases and M increases due to sustained inflow, r_c expands, encompassing more of the surrounding gas and deepening the inflow zone.

This creates a feedback mechanism:

$$\text{Inflow} \rightarrow \text{Mass Growth} \rightarrow \uparrow r_c \rightarrow \text{More Inflow},$$

with no need for merger events or external triggers. Gravitational metric inflow acts as a cosmological conveyor, channeling diffuse gas into the central structure and enabling self-organized galaxy formation.

D. Nested Spiral Structures Across Epochs

Figure 2 illustrates two spirals generated at different epochs under this model. The inner spiral (blue) forms at $z = 5$ around a seed mass of 5×10^{38} kg. As inflow continues, the mass increases and r_c grows. By $z = 0.5$, the inflow zone has expanded significantly, resulting in a second, more extended spiral (red) around the matured bulge of 2×10^{40} kg.

This mechanism can repeat over time, producing layered, self-consistent spiral systems. Each nested spiral reflects a distinct phase of the galaxy's inflow history, naturally structured by metric dynamics.

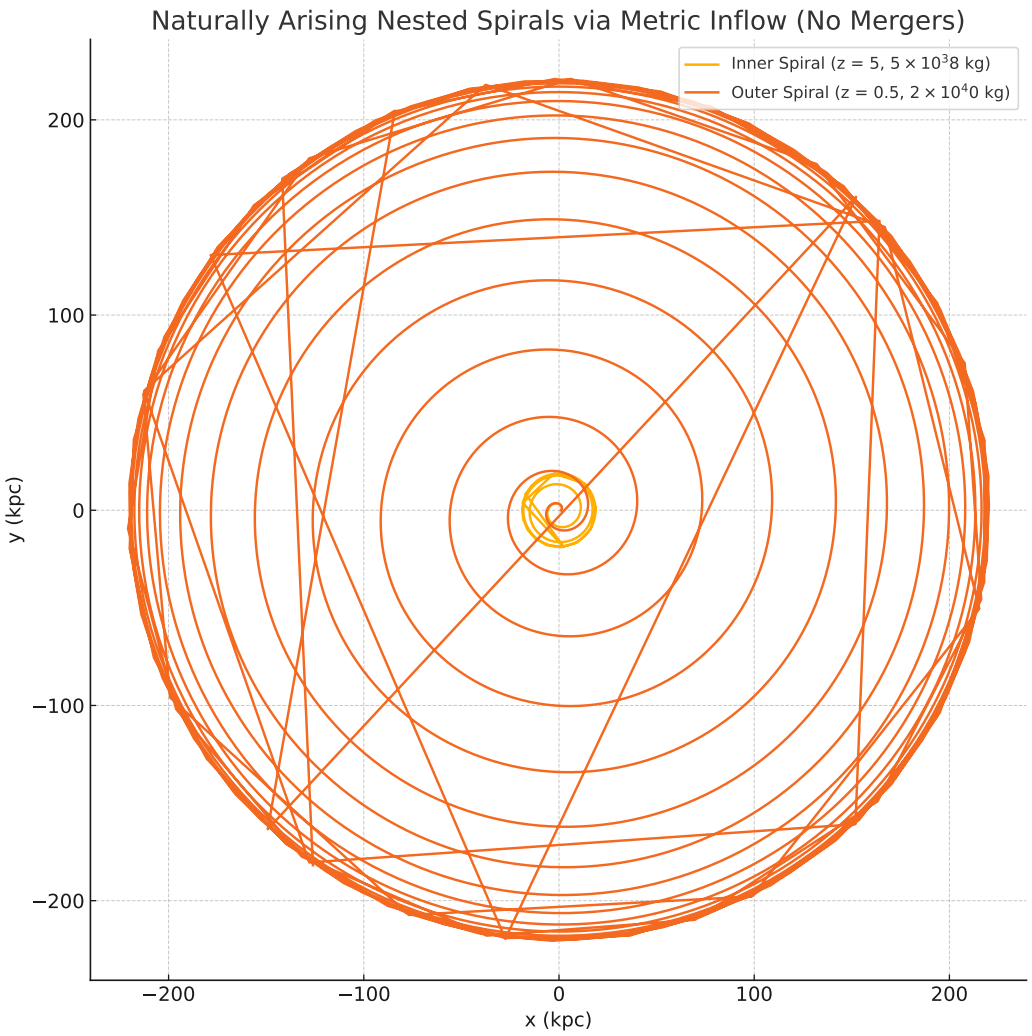

FIG. 2. Naturally nested spiral structures arising from gravitational metric inflow at two cosmic epochs. The inner spiral (blue) forms at redshift $z = 5$ around a seed mass of 5×10^{38} kg. Gravitational attraction is modeled as inward flow of the metric itself, carrying gas into the center along spiral paths. As the central mass increases and the Hubble parameter $H(z)$ decreases, the critical radius r_c grows, enlarging the inflow zone. At $z = 0.5$, the grown bulge of 2×10^{40} kg gives rise to an extended outer spiral (red). The model requires no mergers and generates nested structures through continuous, self-regulated gravitational flow.

E. Implications for Galactic Morphology

This framework suggests a new interpretation of galactic spiral structure:

- Nuclear and extended spirals arise from temporally separated inflow epochs.
- Bulges form as the endpoint of inflow, not via merger-driven collapse.

- Spiral structure directly traces the dynamics of the metric itself, rather than arising from internal instabilities or interactions.

This metric-based approach provides a natural explanation for observed nested spirals and ring structures, reframing galactic formation as a gravitationally self-sustaining process emerging from the evolution of the universe's expansion and its local response to mass accumulation.

F. Spiral Geometry as a Cosmological Probe

In the metric inflow framework, the geometry of spiral structure is not incidental but fundamental. Spiral arms trace the trajectory of spacetime itself, flowing inward under gravity with both radial and azimuthal components. This spiral form is governed by the ratio of the effective radial inflow velocity to the azimuthal orbital velocity of the metric:

$$\tan(\alpha_L(r)) = \frac{|\vec{v}_{\text{rad,eff}}|}{|\vec{v}_{\text{orb}}|} = \frac{\sqrt{\frac{2GM}{r}} - H_z r}{\sqrt{\frac{3}{2}\left(\sqrt{\frac{2GM}{R}} - H_z R\right)^2 - \left(\sqrt{\frac{2GM}{r}} - H_z r\right)^2}}, \tag{6}$$

where M is the mass of the central bulge, R is a reference radius (e.g., bulge radius), and H_z is the Hubble parameter at the time the spiral structure formed.

Given this relationship, one can treat the observed pitch angle $\alpha_L(r)$ of a galaxy's spiral arm as a direct probe of the cosmic expansion rate at its time of formation. Specifically:

- From high-resolution imaging, the spiral structure can be extracted and the pitch angle measured as a function of radius.
- With estimates of the central mass M and a known reference radius R, the full right-hand side of Eq. (6) can be inverted numerically to solve for H_z.
- This yields an effective estimate of the Hubble parameter at the epoch when that spiral layer formed.

Furthermore, when this analysis is combined with the galaxy's optical redshift z_{opt}, one can potentially reconstruct the function $H(z)$ empirically—entirely from observed galaxy morphology and spectroscopy. Each spiral structure effectively serves as a timestamped imprint of the metric dynamics that created it.

Unlike standard candles or chronometers, this method uses galactic morphology as a direct fossil record of cosmic expansion. Repeated across spiral layers and multiple galaxies, this approach could allow independent reconstruction of the $H(z)$ relation—providing a powerful new observational test for cosmology and gravitational theory.

VI. POTENTIAL VOLUME OF $H(z)$ DATA FROM ROTATION CURVES AND SPIRAL FITS

A major advantage of the gravitational metric inflow model is that observable galactic features—such as spiral structure and rotation curves—can directly encode the Hubble parameter $H(z)$ at the epoch when the structure formed. This enables each spiral galaxy to serve as a cosmological chronometer.

A. Rotation Curves as Chronometers

In the metric inflow framework, orbital velocity profiles are determined by a balance between gravitational inflow and cosmological expansion. As shown in Eq. (II F 2), the orbital velocity at radius r depends on the central mass M, the bulge radius R, and the Hubble parameter H_z. Fitting observed rotation curves with this model allows extraction of an effective $H(z)$ at the time the rotation pattern was established.

Because high-quality rotation curve data exist for thousands of galaxies from HI and optical surveys (e.g., THINGS, SPARC, WHISP), this method has significant scaling potential.

B. Spiral Geometry as Chronometers

Similarly, the pitch angle of spiral arms, measurable from high-resolution imaging (e.g., SDSS, DECaLS, HST, JWST), can be inverted to yield $H(z)$ using the metric inflow velocity equations. Multiple spiral layers in a galaxy may correspond to successive epochs of structure formation, enabling multi-redshift $H(z)$ measurements from a single object.

C. Estimated Data Volume

Table I compares the potential number of $H(z)$ points that can be extracted from current and future methods.

TABLE I. Estimated number of $H(z)$ data points obtainable from various methods.

Method	Estimated Data Points	Redshift Range	Source/Comments
BAO (standard)	20–30	$0.1 < z < 2.3$	SDSS, eBOSS, DESI
Cosmic chronometers	$\sim$30	$0.1 < z < 2.0$	Galaxy spectra
Strong lensing delays	$\sim$5	$0.5 < z < 2.5$	Quasar lenses
CMB model fit	1	$z \approx 1100$	Planck
Rotation curves (this work)	10,000–100,000	$z = 0.01$–1.5	HI + optical kinematics
Spiral fits (this work)	100,000–1,000,000	$z = 0.01$–6	Optical imaging morphology

D. Implications

While standard cosmology relies on a limited number of heterogeneous, often model-dependent $H(z)$ measurements, the metric inflow model provides a direct and scalable alternative. By using morphology and dynamics alone—without invoking dark matter—hundreds of thousands of $H(z)$ measurements may become accessible.

This methodology enables independent reconstruction of the cosmic expansion history, offering a new observational probe of cosmology and gravity.

VII. DISCUSSION AND CONCLUSIONS

We have proposed a new method for reconstructing the cosmic expansion history $H(z)$ using spiral structure and galaxy rotation curves within the framework of gravitational metric inflow. In this model, spacetime itself flows inward in a spiral pattern under the influence of a central gravitational source and the large-scale cosmological expansion. This flow defines both the rotational dynamics of galaxies and their spiral geometry, without invoking extended dark matter halos.

A. Key Findings

- We derived closed-form expressions for the orbital velocity and spiral pitch angle of the metric inflow, which depend on three quantities: the central bulge mass M, a reference radius R, and the Hubble parameter H_z at the time the structure formed.
- This approach can scale to thousands or even millions of galaxies, offering orders of magnitude more $H(z)$ data points than current standard candles, chronometers, or BAO methods.

B. Implications for Cosmology

The metric inflow framework recasts galactic structure as a direct imprint of cosmic expansion, treating spiral galaxies as self-contained cosmological observatories. Unlike standard methods, which rely on statistical samples, distance ladders, or model-dependent time delays, this approach uses only imaging, dynamics, and redshift data—available for a vast number of galaxies.

If validated across diverse galaxy types and redshifts, this model could:

1. Provide a high-resolution reconstruction of the Hubble function $H(z)$ across cosmic time, especially at low to intermediate redshifts.
2. Offer a dark-matter-free explanation for flat and rising rotation curves, directly linking local dynamics to cosmological expansion.
3. Open the door to reinterpreting spiral structure as a metric phenomenon—emergent from gravitational and cosmological flows rather than local instability.

C. Open Questions and Future Work

While promising, the model introduces new theoretical assumptions—particularly the existence of a Lagrangian metric inflow with a spiral geometry. Several open questions remain:

- What fundamental theory underlies the assumed spiral inflow behavior of spacetime?
- How does this framework generalize to galaxies with irregular or non-spiral morphology?
- Can this approach consistently explain galaxy clustering, lensing, and large-scale structure without dark matter?

- How robust is the inversion of spiral and velocity data under observational uncertainties and non-spherical mass distributions?

D. Conclusion

We propose that galactic morphology and kinematics—long considered the domain of astrophysics—may offer direct and scalable access to cosmological information. If validated, this method has the potential to redefine how we measure the expansion of the universe and understand the link between gravity and cosmology.

Appendix A: Spiral plots with the improved rotation curve vectors

REFERENCES

[1]de Haas, E. P. J. (2018). A 'constant lagrangian' rmw-rss quantified fit of the galaxy rotation curves of the complete sparc database of 175 ltg galaxies. *viXra.org:Astrophysics*, page https://vixra.org/abs/1908.0222.

[2]de Haas, E. P. J. (2025a). One single metric model's unifying perspective on four issues with galactic dynamics: B-tf relation, rotation curves, spirals and smbh-growth. *viXra:2506.0097*. preprint https://vixra.org/abs/2506.0097.

[3]de Haas, E. P. J. (2025b). Space quantum gravity. *Journal of High Energy Physics, Gravitation and Cosmology*, 11(2).

[4]de Haas, E. P. J. (2025c). Spiral arms as fossil tracers of cosmic expansion: Inferring galaxy formation epochs from pitch angle morphology. *viXra:2507.0021*. preprint https://https://vixra.org/abs/2507.0021.

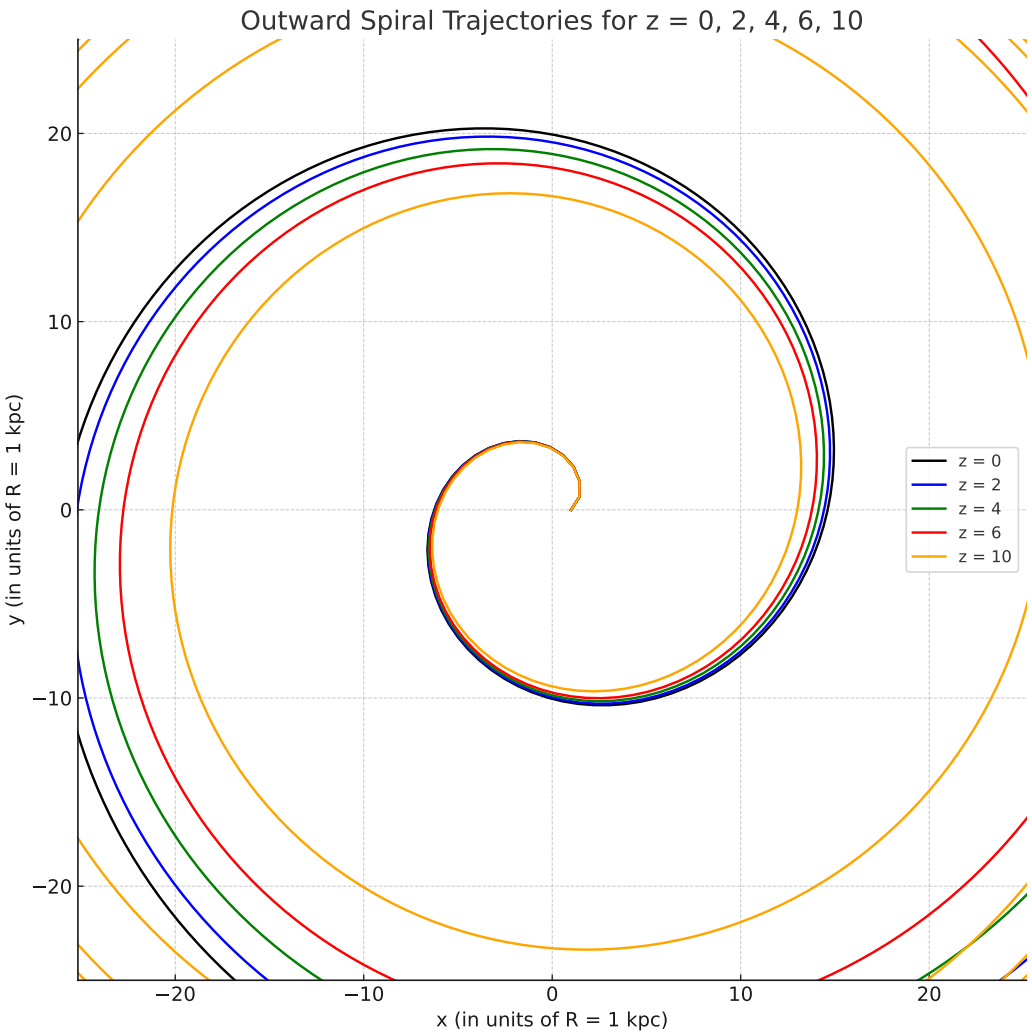

FIG. 3. Outward spiral trajectories of space motion for redshifts $z = 0, 2, 4, 6$, and 10, computed in a Planck 2018 ΛCDM cosmology. Each trajectory starts at a reference radius of $R = 1$ kpc and evolves outward under the effective velocity $\vec{v}_L = \vec{v}_{\text{orb}} + \vec{v}_{\text{rad,eff}}$, which combines the orbital and radial infall components of space motion around a galactic bulge of mass $M = 2 \times 10^{40}$ kg. The motion terminates at the critical radius r_c, where the effective radial velocity vanishes and the trajectory becomes purely tangential. The computed critical radii are: $r_c(z = 0) = 4.64$ kpc, $r_c(z = 2) = 9.00$ kpc, $r_c(z = 4) = 11.64$ kpc, $r_c(z = 6) = 13.11$ kpc, and $r_c(z = 10) = 20.86$ kpc.

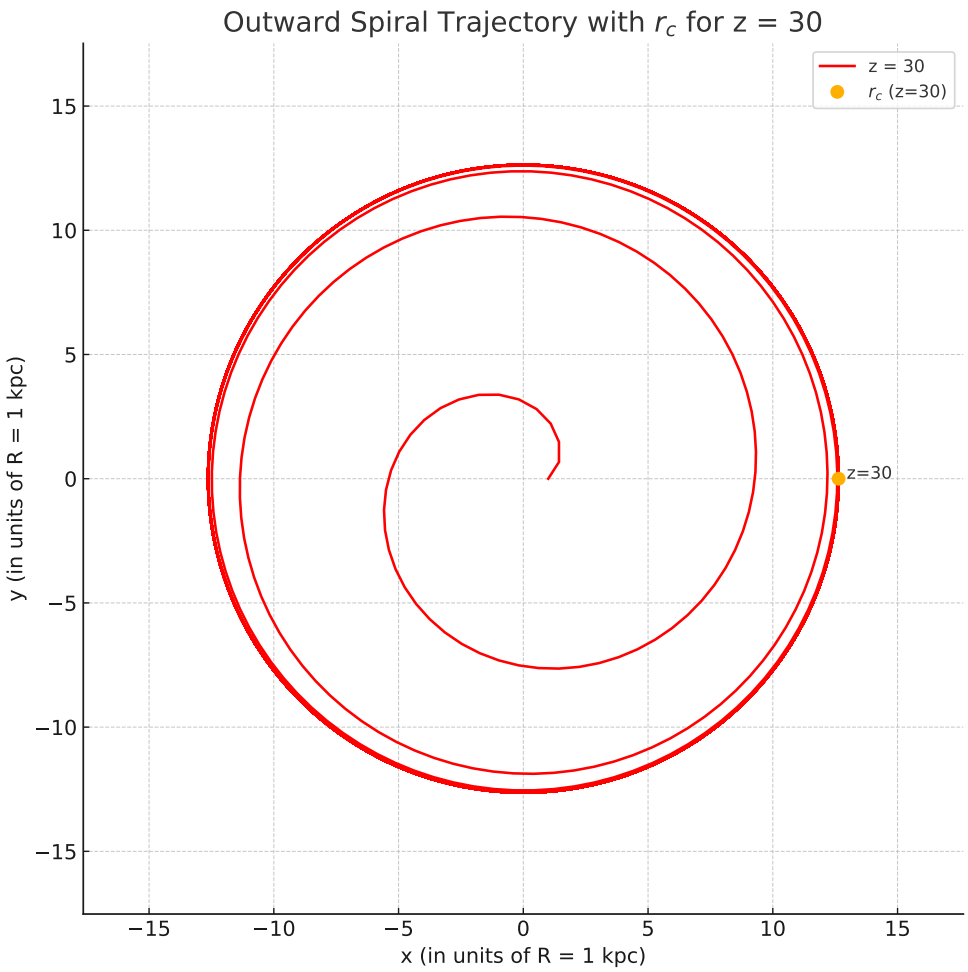

FIG. 4. Outward spiral trajectory of space motion at redshift $z = 30$, starting from a reference radius $R = 1$ kpc and terminating at the critical radius r_c, where the effective radial velocity vanishes and motion becomes purely tangential. The dynamics are governed by a combination of infalling and rotational velocities under Planck 2018 ΛCDM cosmology. The system models a galactic bulge with mass $M = 2 \times 10^{40}$ kg. The critical radius r_c is marked with a red dot.

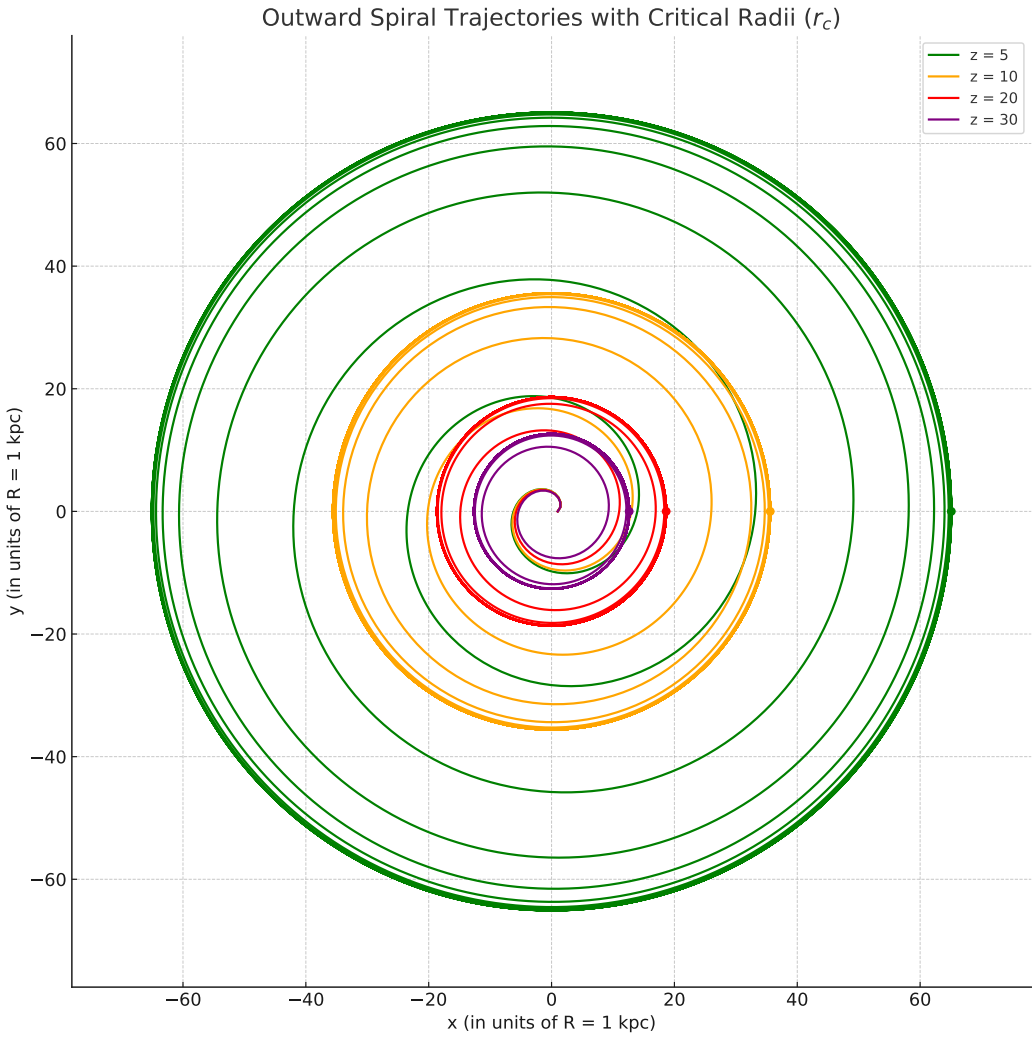

FIG. 5. Outward spiral trajectories of space motion for redshifts $z = 5$, 10, 20, and 30, computed under Planck 2018 ΛCDM cosmology. Each trajectory begins at a reference radius of $R = 1$ kpc and proceeds outward following the velocity vector $\vec{v}_L = \vec{v}_{\text{orb}} + \vec{v}_{\text{rad,eff}}$, until reaching the critical radius r_c where the radial velocity component vanishes and the flow becomes purely tangential. The system models a galactic bulge with mass $M = 2 \times 10^{40}$ kg. The computed values of r_c are: $r_c(z = 5) = 13.44$ kpc, $r_c(z = 10) = 20.86$ kpc, $r_c(z = 20) = 32.58$ kpc, and $r_c(z = 30) = 39.75$ kpc.

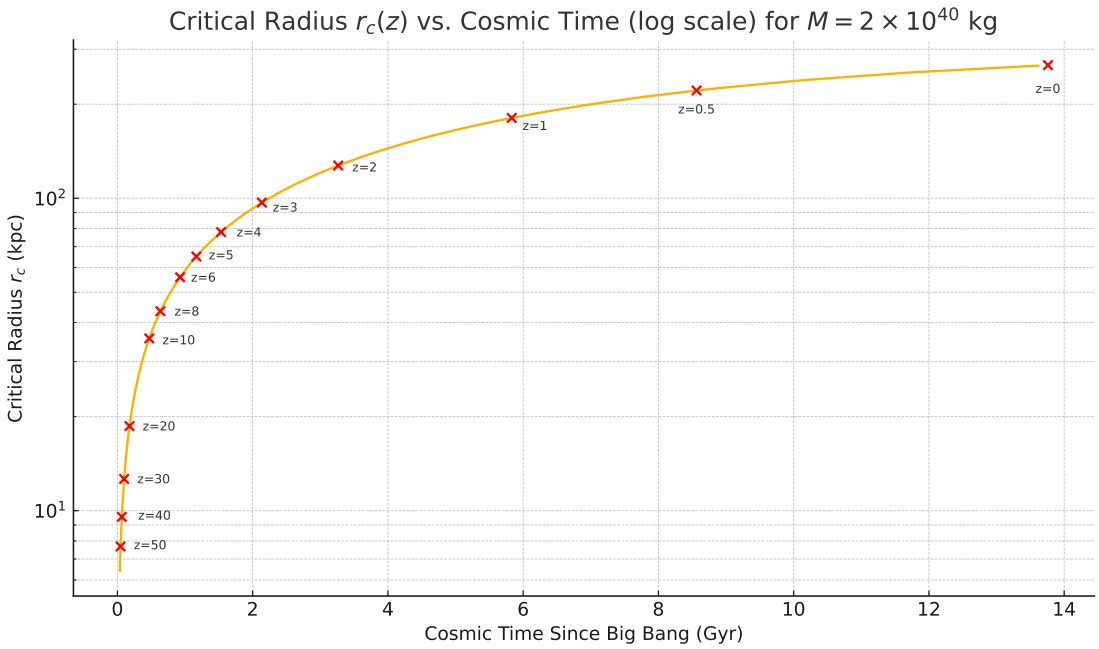

FIG. 6. Critical radius $r_c(z)$ as a function of cosmic time (in Gyr) for a gravitational potential sourced by a galactic bulge of mass $M = 2 \times 10^{40}$ kg. The critical radius is defined as the distance at which the effective radial space flow velocity vanishes, given by $r_c = \left(\frac{2GM}{H(z)^2}\right)^{1/3}$. The curve shows r_c evaluated under Planck 2018 ΛCDM cosmology using a logarithmic scale for r_c. Red dots indicate the critical radius at specific redshifts: $z = 0$, 0.5, 1, 2, 3, 4, 5, 6, 8, 10, 20, 30, 40, and 50. This visualizes how the cosmic expansion rate shapes the spatial extent of gravitational inflow over time.